Biomaterials Science

ROYAL SOCIETY OF CHEMISTRY

PAPER

View Article Online
View Journal | View Issue

Cite this: *Biomater. Sci.*, 2024, **12**, 2282

Natural polyphenolic antibacterial bio-adhesives for infected wound healing†

Hengjie Zhang,[a] Yuqi Feng,[a] Tianyou Wang,[a] Jianhua Zhang,[a] Yuxian Song,[a] Jing Zhang,[b] Yiwen Li,[a] Dingzi Zhou*[b] and Zhipeng Gu *[a]

Received 29th December 2023,
Accepted 7th February 2024

DOI: 10.1039/d3bm02122j

rsc.li/biomaterials-science

Bio-adhesives used clinically, commonly have the ability to fill surgical voids and support wound healing, but which are devoid of antibacterial activity, and thus, could not meet the particular needs of the infected wound site. Herein, a series of natural polyphenolic antibacterial bio-adhesives were prepared *via* simple mixing and heating of polyphenols and acid anhydrides without any solvent or catalyst. Upon the acid anhydride ring opening and acylation reactions, various natural polyphenolic bio-adhesives could adhere to various substrates (*i.e.*, tissue, wood, glass, rubber, paper, plastic, and metal) based on multi-interactions. Moreover, these bio-adhesives showed excellent antibacterial and anti-infection activity, rapid hemostatic performance and appropriate biodegradability, which could be widely used in promoting bacterial infection wound healing and hot burn infection wound repair. This work could provide a new strategy for strong adhesives using naturally occurring molecules, and provide a method for the preparation of novel multifunctional wound dressings for infected wound healing.

1. Introduction

Wound infection, as a result of bacterial growth in damaged skin wounds, includes wound bleeding, fever and inflammation, pain and redness, delayed healing, and increased exudate, which significantly impacts human safety and quality of life.[1–7] So, the care and rapid healing of bacterial infection wounds were facing great challenges.[8–11] Therefore, a new multifunctional anti-infective wound dressing system, which has good antimicrobial ability is greatly required.[12–15] Bio-adhesives, as new medical adhesives, which are effective candidates to replace sutures, have the advantages of effective treatment of wounds, good biocompatibility, and provide a suitable environment for cell growth and tissue repair.[16–19] Therefore, it is important and effective to construct a new multifunctional bio-adhesive wound dressing for infected wounds.

One potential strategy to address this issue is to use natural plants and extracts as a source of inspiration.[20–23] In nature, numerous plant extracts (*i.e.*, green tea, cellulose, lignin, tannins, pomegranate peel, and grape seeds) have excellent anti-oxidant and anti-infective properties, which inspired us to further develop new wound dressings by logical selection and use of widely existing natural molecules.[12,24–26] Natural polyphenols, are a natural biomolecule found to exist in various plants, and they have been widely designed in forms such as carbon dots, nanoparticles, and hydrogels for wound healing in recent years.[27–32] Polyphenols benefit from their abundant catechol and triphenol groups, and could exhibit excellent antioxidant and anti-infective properties, and also exhibit a good adhesion ability to bio-tissues through various strong interactions.[33,34] For example, catechol and synthetic catechol-based adhesives have been prepared by various oxidative polymerization and crosslinking reactions, which have been used in energy, industrial, and biomedical applications.[35–37] Therefore, it is extremely important for us to prepare novel polyphenol bio-adhesives for the treatment of infected wounds by selecting new natural adapted biological molecules.

Acid anhydrides, as commercialized molecules, could be prepared as natural product molecules by using biomass-derived molecules.[38–40] For example, the commonly used monomer, maleic anhydride (MA) could be prepared using cellulose and lignin for a highly efficient biobased synthesis, which has been used in the preparation of eco-friendly cellulose and other polymer materials.[41,42] In addition, numerous anhydrides have been used in the synthesis of various bio-polymers (*i.e.*, block copolymers, polymer vesicles, and polymeric peptides) using ring opening polymerization (ROP) reactions, which could be used for biological applications, including antibacterial therapy,[43] drug delivery,[44] and cell therapy.[45] Therefore, we speculate that anhydride molecules could serve

[a]*College of Polymer Science and Engineering, State Key Laboratory of Polymer Materials Engineering, Sichuan University, Chengdu 610065, China. E-mail: guzhipeng2019@scu.edu.cn, drzdz@scu.edu.cn; Tel: +86 028-85401066*
[b]*West China School of Public Health and West China Fourth Hospital, Sichuan University, Chengdu 610065, China*

† Electronic supplementary information (ESI) available. See DOI: https://doi.org/10.1039/d3bm02122j

as natural adapted biological molecules to prepare new bio-adhesives by combining them with natural polyphenols, which could then be used for the treatment of wound infections healing.

Herein, we report on a series of antibacterial bio-adhesives which were prepared *via* the natural polyphenol and acid anhydride-crosslinking (PAC) reaction (acid anhydride ring opening and acylation reactions) with a simple mixture and heating without any solvent or catalyst (Fig. 1a). Various typical natural polyphenols (extracts), and various acid anhydrides were examined. After heating, the natural polyphenolic adhesives could induce strong adhesion onto various substrates based on multi-interactions. In addition, these as-prepared adhesives showed a rapid hemostatic performance, great biocompatibility, and appropriate biodegradability. Also, the as-prepared bio-adhesives exhibited excellent antibacterial and anti-infective abilities, which could effectively promote the wound healing of bacterial infection and hot burn infection. We believe that this work can provide a new strategy for robust adhesives using naturally occurring molecules, and provide a method for the preparation of novel multifunctional wound dressings for infected wound healing.

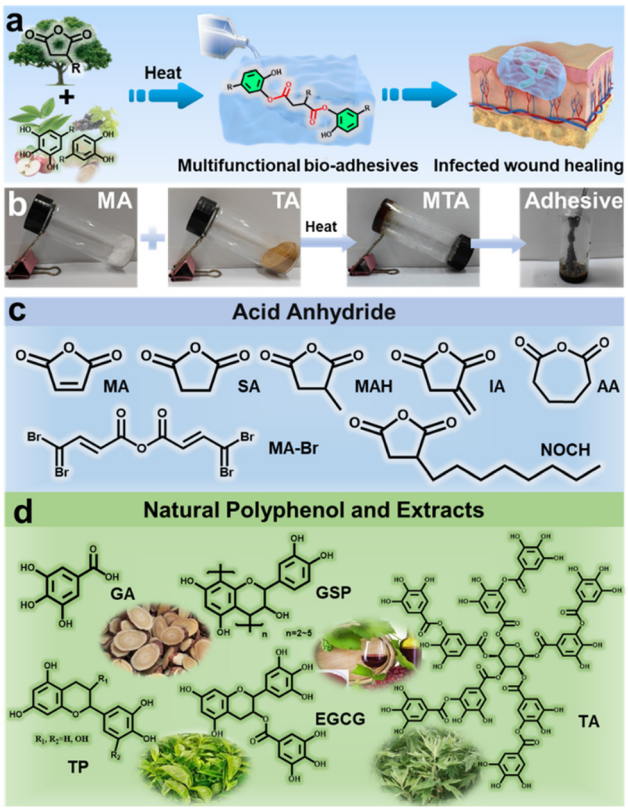

Fig. 1 Natural polyphenolic bio-adhesives with great antibacterial activity for infected wound healing. (a) Schematic illustration and (b) optical photograph of the natural polyphenol-acid anhydride bio-adhesives. (c) Chemical structure formulas of acid anhydrides. (d) Chemical structure formulas of natural polyphenols (extracts).

2. Experimental section

2.1 Materials

Tannic acid (TA, 99%), gallic acid (GA, 99%), maleic anhydride (MA, 99%), succinic anhydride (SA, 99%), methyl succinic anhydride (MAH, 99%), itaconic anhydride (IA, 98%), adipic anhydride (AA, 98%), bromomaleic anhydride (MA-Br, 98%), and *N*-octylsuccinic anhydride (NOCH, 98%) were purchased from Aladdin Biochemical Technology Co. Ltd (Shanghai, China). Epigallocatechin gallate (EGCG, 98%), tea polyphenol (TP, 70%), grape seed polyphenol (GSP, 70%), red wine extract (RWE, 50%–70%), mugwort polyphenol extract (MPE, 50%–70%), phyllanthus polyphenol extract (PPE, 50%–70%) were obtained from DASF Bio-Technology Co. Ltd (Nanjing, China). The chemical reagents did not undergo any treatment before use.

2.2 Synthesis of natural polyphenolic bio-adhesives

The natural polyphenolic bio-adhesives were synthetized *via* the acid anhydride ring opening and acylation reactions at 100 °C between natural polyphenols (extracts) and acid anhydride molecules. Specifically, bio-adhesives were obtained by mixing 10 mol acid anhydrides and 1 mol natural polyphenols (extracts) at 100 °C, and then after subsequent cooling the bio-adhesive adhesives were obtained. Adjusting the types of natural polyphenols (extracts) and acid anhydrides was used to improve the adhesive ability. Finally, MA and TA were selected as candidates for synthesizing MTA bio-adhesives. Specifically, the MTA bio-adhesive was obtained by mixing 10 mol MA and 1 mol TA at 100 °C.

2.3 Adhesion testing

First, various substrates including rubber, glass, wood, paper, PET, Cu, Al, Fe, and skin were procured from local markets. Then, the adhesion force and strength were measured *via* the tensile testing machine (the force transducer parameter was 500 N; stretching speed was 10 mm min^{-1}). Specifically, 300 μL natural polyphenolic adhesives were uniformly coated on the substrate surface (area: 25 mm × 25 mm). The adhesion of the samples was tested by pressing them and then loading them onto a tensile machine and stretching them until they broke. The maximum tensile force (F_{max}) was recorded and the bond strength was calculated by dividing F_{max} by the coated area. Moreover, some destroyed tissues (*i.e.*, heart, liver, lung, spleen, and stomach) were bonded and characterized by MTA bio-adhesives, and their adhesion interface was observed using SEM.

2.4 Antibacterial testing

Firstly, to estimate the numbers of surviving bacteria, natural polyphenolic bio-adhesives were placed into the *Escherichia coli* (*E. coli*) and *Staphylococcus aureus* (*S. aureus*) bacterial solution (200 μL, 10^8 CFU mL^{-1}) at 37 °C for 24 h and the counts were acquired by measuring the optical density at 600 nm using a fluorometer. To estimate the morphology of live and dead bacteria, the cultured suspension was scanned

by SEM and a fluorescence microscope. The antibacterial of the bio-adhesives were evaluated using the zone of inhibition (ZOI) test. In brief, 100 μL of bacteria solution (10^8 CFU mL^{-1}) was pipetted onto plates containing lysogeny broth (LB) agar culture medium and distributed evenly. Then the natural polyphenolic adhesives were placed into the plates and incubated at 37 °C for 24 h. The ZOI was defined by examining the transparent area around the natural bio-adhesives on the agar surface.

2.5 Hot burn infection wound healing

To evaluate the adhesion and antibacterial applications of MTA adhesives, a rat hot burn infection wound model was established. Firstly, the rats (20 ± 5 g, Chengdu Dashuo Co., Ltd) were selected and disinfected, and they were then randomly divided into four groups (commercial medicine dressing, MTA adhesives, MA and TA powder, and a control). Then, the skin wound was prepared with a hot metal stick, and ~100 μL of MTA bio-adhesives were dropped into the wound, and pressed to produce adhesion. The control group did not have any treatment, and the commercial medicine group had the purchased commercial medicine dressing (Cofoe, G1308, China) applied. Finally, the rats were fed normally and the wound area was photographed every day. The tissues were collected after different times and cultured for bacteria growth. Moreover, all the animals were sacrificed and the above histopathological examination performed, which was estimated with image analysis software ImageJ (USA).

3. Results and discussion

3.1 Preparation and characterization of natural polyphenolic bio-adhesives

The proposed natural polyphenolic bio-adhesives were prepared *via* the natural polyphenol and acid anhydride-crosslinking (PAC) reaction (acid anhydride ring opening and acylation reactions) at 100 °C between natural polyphenols (extracts) and acid anhydride molecules. For example, the MTA natural adhesives were formed using the covalent (*i.e.*, acid hydride ring opening and acylation reactions) and non-covalent (*i.e.*, hydrogen bonding) crosslinking of TA and MA under heating conditions, which showed excellent adhesion properties as the temperature gradually decreased (Fig. 1b). In addition, the versatility of this method was demonstrated by using different types of acid anhydrides to react with natural polyphenols (extracts) (Fig. 1c, d, and Fig. S1†). Then, the ratio of TA and MA to form natural adhesives was further explored as shown in Fig. 2a and Fig. S2,† and the results showed that the MTA adhesives formed when the ratio of TA to MA was about 1 mol : 10 mol. Moreover, the injectability, shaping ability and self-healing ability were examined at different temperatures (Fig. 2b). For example, the MTA natural adhesives could be injected through a syringe after heating and it could be molded into different shapes. Meanwhile, the round and square MTA natural adhesive was sliced in half, and then these

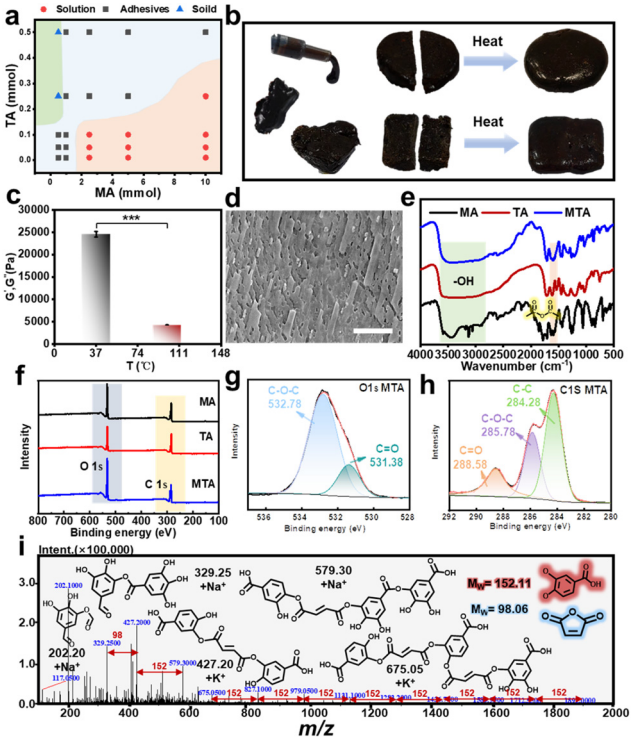

Fig. 2 Characterization of natural polyphenolic bio-adhesives. (a) Phase diagram of natural polyphenolic adhesives with different TA and MA ratios. (b) Self-healing behavior and injectability of the MTA natural bio-adhesives. (c) Dynamic storage modulus (*G′*) of the MTA natural bio-adhesives at different temperatures. (d) SEM image of MTA natural adhesives (scale bar: 10 μm). (e) FTIR spectra of TA, MA, and the MTA natural bio-adhesives. (f) XPS survey spectra of TA, MA, and the MTA natural bioadhesives. (g) The O 1s peaks and (h) the C 1s peaks in XPS spectra of MTA natural bio-adhesives. (i) The ESI-MS spectrum of MTA natural bio-adhesives. *p < 0.05, **p < 0.01, ***p < 0.001.

adhesives were used in close contact under 100 °C for 10 min to form a complete adhesive interface. In addition, the rheological properties of the MTA natural adhesives at different time were verified using a dynamic rheometer. As shown in Fig. 2c and Fig. S3,† the energy storage modulus G' of the MTA natural adhesives at 37 °C was much higher than that at 100 °C, which may be because the hydrogen bonding of the MTA natural adhesives would be disrupted at higher temperatures. When the temperature rises, the hydrogen bond force would decrease, resulting in a significant decline of G'. Moreover, the resulting multifunctional MTA natural bio-adhesives were further characterized by SEM, and as shown in Fig. 2d and Fig. S4,† it was found that the MTA natural bio-adhesive had a denser microporous structure when compared to those of the MA and TA monomers, which further proved that the crosslinked adhesive structures were formed after the PAC reaction.

Moreover, the chemical structure of the natural bio-adhesives was studied by FT-IR, XPS, and ESI-MS. From Fig. 2e, the typical peaks corresponding to the functional groups of TA and MA could be observed in the natural adhesive, where the characteristic peaks at ~3500 cm^{-1} were

attributed to the phenolic group of TA, and the characteristic peaks at ~1600 cm^{-1} were attributed to the carbonyl groups in MA. In addition, as demonstrated in the XPS survey result (Fig. 2f), we found the appearance of C and O elements within MTA adhesives, and when compared with MA, a significant decrease of the average content of C═O (288.58 eV) could also be observed, and C–O–C (285.78 eV) was observed in MTA adhesives, which was similar to the peak separation found in TA. These results further proved that MA undergoes ring opening reaction and reacted with polyphenols (extracts) to form adhesives (Fig. 2g, h and Fig. S5†). Moreover, the reaction mechanism of natural polyphenolic bio-adhesives was identified by ESI-MS spectroscopy. It was noted that the combination of TA and MA was observed in several emerging *m*/*z* peaks, which could confirm the possible chemical structure of the MTA crosslinking reaction (Fig. 2i and Fig. S6†). Together, these results showed the successful preparation of natural polyphenolic bio-adhesives, which could be used for further adhesive applications.

3.2 Adhesion capability of natural polyphenolic bio-adhesives

The adhesive properties of natural polyphenolic bio-adhesives were studied qualitatively and quantitatively using various substrates. As expected, the prepared MTA natural bio-adhesives showed universal adhesion properties on different substrates, which included wood, rubber, glass, plastics, cellulose, and metals (Fig. 3a). And the details of the quantitative measurement are shown in Fig. 3b and Fig. S7.† In short, the MTA natural adhesives were heated to soften them sufficiently, and they were then evenly coated on various substrates, then another substrate was covered with natural polyphenolic bio-adhesives, pressed tightly, and allowed to cool. Then, the prepared samples were placed on the universal tensile testing machine until they broke. As expected, the MTA adhesives showed strong bonding strengths with different substrates (*i.e.*, Al, Fe, Cu, glass, PET, paper, wood, and pig skin) see Fig. 3c and d. For instance, the F_{max} of wood was ~800 N and the adhesive strength was ~500 kPa. Noting that the pig skin exhibited strong adhesion performances (~300 kPa), which met the requirements of bio-tissues according to previous reports in the literature.[19,46–48] So, the excellent tissue adhesion performance of the MTA natural bioadhesives was further verified by using a tissue cutting repair process. In brief, various tissues including heart, liver, spleen, stomach, and kidney were made into a 5 mm wound using scissors, and the MTA natural bio-adhesives were applied onto the wound surface to achieve adhesion. As shown in Fig. 3e, it could be clearly observed that the MTA natural bioadhesives could effectively adhere to the tissue wounds. Moreover, the SEM cross-sectional images showed the tight micro interface between the MTA natural adhesives and tissue. It was also found that there was no significant stratification between the MTA natural adhesives and different tissues (*e.g.*, liver, spleen), which further indicated that the prepared MTA bio-adhesives had an excellent tissue adhesion performance (Fig. 3f). Finally, the

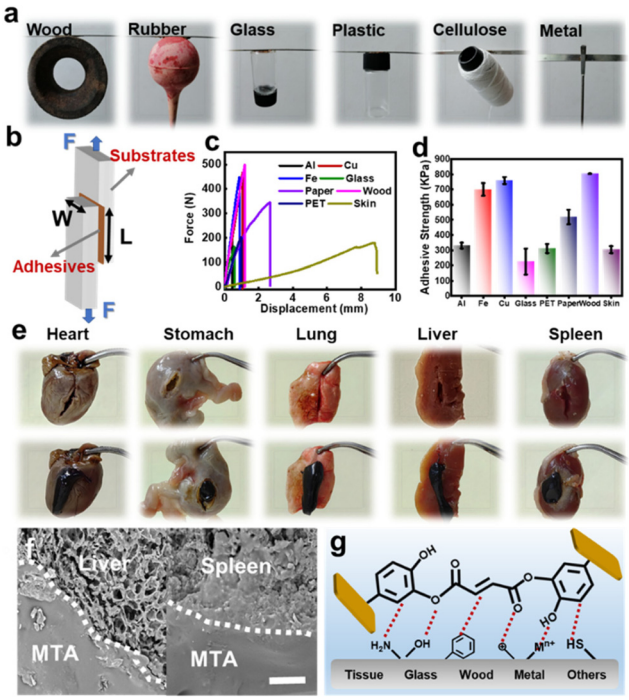

Fig. 3 Universal adhesion capability of natural polyphenolic bio-adhesives. (a) Optical images of MTA natural bio-adhesives adhesion with various substrates. (b) Schematic diagram of mechanical tensile testing. (c) F_{max} and (d) adhesive strength of the MTA natural bio-adhesives with various substrates. (e) Representative optical photographs demonstrating the adhesion interfaces between MTA natural bio-adhesives and different tissues. (f) Representative SEM images showing the adhesion interfaces between MTA natural bio-adhesives and different tissues (scale bar: 30 μm). (g) The adhesion mechanism of MTA natural bio-adhesives with various substrates.

adhesion mechanism of the MTA natural bio-adhesives was further discussed and analyzed. Firstly, we believe that the multiple catechol groups could undergo various interactions with different substrate surfaces. For example, catechol groups could interact with tissues through noncovalent interactions (*i.e.*, electrostatic interactions, hydrogen bonds, cation–π interactions) and covalent interactions (*i.e.*, Michael addition and Schiff base reactions).[43–45] In addition, acid anhydrides, as the crosslinking agents and adapting key units of natural polyphenol (extracts), could introduce more covalent and non-covalent interactions (*i.e.*, the amidation reaction, hydrogen bonds, the ring opening reaction, electrostatic interactions, and so on), which would further enhance the adhesion ability of the MTA natural bio-adhesives with tissues (Fig. 3g). Therefore, these results confirmed that the natural polyphenolic adhesives had an excellent universal adhesion performance, which could be further used for adhesive tissue applications.

3.3 Hemostatic performances of natural polyphenolic bio-adhesives

Then, to evaluate the hemostatic performance of MTA natural adhesives, the heart, liver, and rat tail injury models were established (Fig. 4a). Firstly, scissors were used to create a

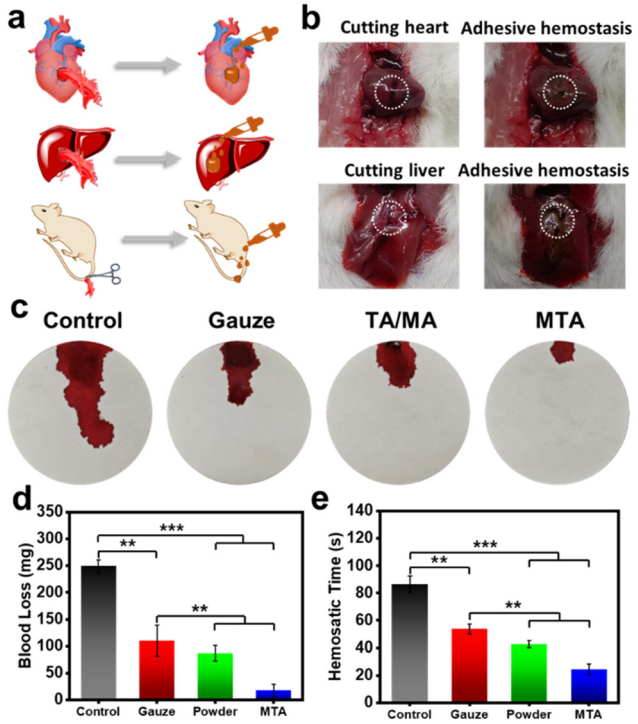

Fig. 4 Hemostatic performances of natural polyphenolic bio-adhesives. (a) Schematic illustration showing the use of natural polyphenolic bio-adhesives for the heart, liver, and rat tail injury models. (b) *In vivo* adhesion of natural polyphenolic bio-adhesives on the cut rat liver and heart. (c) Optical images of blood loss after different treatments. (d) The hemostatic adhesion evaluation was performed by recording blood loss. (e) The hemostatic adhesion evaluation was performed by recording hemostatic time. *$p < 0.05$, **$p < 0.01$, ***$p < 0.001$.

standard liver and heart wound (4 mm) injury model, and the MTA natural bio-adhesives were applied on the wound surface. From Fig. 4b, it can be seen that the MTA adhesives could effectively adhere to the tissue surface to block blood flow and achieve rapid hemostasis. Then, the excellent hemostatic performance of MTA natural bio-adhesives was quantitatively determined using the tail hemostasis models. In detail, the tails of the rats were cut off to make them bleed, and then different groups (*i.e.*, control, gauze, TA/MA powder, and MTA bio-adhesives) were used for hemostasis treatment. The weight of the blood absorbed was measured using a filter paper until the bleeding stopped, and the blood hemostasis time was recorded (Fig. 4c and Fig. S8†). From Fig. 4d, it can be seen that the MTA natural bio-adhesives could quickly stop bleeding and had a shorter hemostatic weight (17.87 ± 11.13 mg) when compared to the control group (248.90 ± 11.99 mg), the gauze group (110.37 ± 29.33 mg) and the TA/MA powder group (87.37 ± 14.41 mg). Meanwhile, the hemostatic time showed a remarkable decrease after applying the MTA natural bio-adhesives when compared to the other groups (Fig. 4e), which was due to the fact that the MTA natural bioadhesives could adhere to the wound surface by various interactions (*i.e.*, the hydrogen bonding interaction). Altogether, all these results showed that the MTA natural bio-adhesives possessed excellent hemostatic properties *in vivo*, which could fulfill the demands for wound healing and tissue bio-adhesion.

3.4 Biocompatibility and biodegradability of natural polyphenolic bio-adhesives

Then, the biocompatibility and biodegradability of the MTA natural bio-adhesives were evaluated. Firstly, the biocompatibility and the cell proliferation activity of NIH 3T3 cells were measured using the alamarBlue assay and live/dead staining. From Fig. 5a, it can be observed that the NIH 3T3 cells incubated with a low concentration of MTA natural bio-adhesives, MA and TA monomers could similarly proliferate with control group, which may be because they have excellent biocompatibility as biomass molecules. Notably, the cell viability remained at ~90% as the concentration increased, measured *via* the alamarBlue assay, which indicated the excellent biocompatibility and cell proliferation activity of the MTA natural bio-adhesives (Fig. 5b).

Moreover, the biodegradability *in vivo* was evaluated by implanting ~100 μL of MTA natural bio-adhesives in the dorsal subcutaneous space of mice, then the rats were fed normally for 8 days, and the biodegradability of the glues was evaluated by measuring the wound area and size at different times (Fig. 5c). As shown in Fig. 5d, e and Fig. S9,† it was found that the MTA bio-adhesives had an appropriate degradation rate,

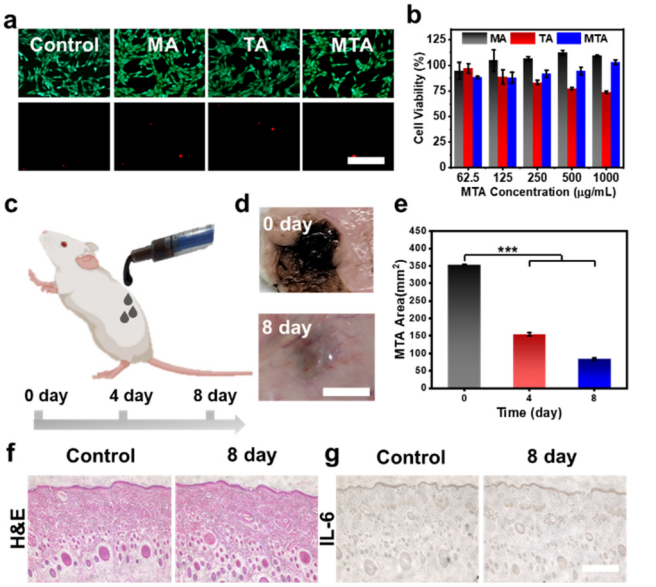

Fig. 5 Biocompatibility and biodegradability of natural polyphenolic bio-adhesives. (a) Cytocompatibility of different groups in the live/dead staining assay of NIH 3T3 cells (scale bar: 50 μm). (b) The NIH 3T3 cell viability with MTA bio-adhesives at different concentrations. (c) Schematic illustration of MTA bio-adhesives subcutaneous injection biodegradability at different times. (d) Optical images of the biodegradability in the dorsal subcutaneous space of mice at day 0 and day 8 (scale bar: 10 mm). (e) The wound area of the dorsal subcutaneous space at different times. (f) The H&E staining and (g) the IL-6 immunohistochemical staining of subcutaneous tissue after 8 days (scale bar: 50 μm). *$p < 0.05$, **$p < 0.01$, ***$p < 0.001$.

and the wound areas of the spaces were 353.56 ± 1.24 mm^2, 154.66 ± 5.02 mm^2, 83.51 ± 3.68 mm^2 at day 0, day 4, and day 8, which was conducive to the use of these natural polyphenolic bio-adhesives *in vivo*. It was noted that there was a slight redness and inflammatory response in the wound tissue, which was consistent with results found in previous reports.[49–51] Moreover, after 8 days, the injection site was removed from the rats for histopathological examination, including hematoxylin–eosin (H&E) and interleukin-6 (IL-6) staining. As shown in Fig. 5f, the H&E staining of the subcutaneous tissue demonstrated that the wounds treated with MTA bio-adhesives after 8 days possessed similar epithelial tissues when compared with the control group. It was found that there was a gradual proliferation and recovery of the subcutaneous tissue after the bio-adhesives treatment, which further indicated that the MTA natural bio-adhesives derived from bio-macromolecules had a lower inflammatory response. In addition, the IL-6 immunohistochemistry analysis showed that there was no more obvious positive expression in the implanted tissue sites of the MTA bio-adhesives, which further demonstrated the acceptable inflammatory stimulation (Fig. 5g). Altogether, the above results demonstrated that the prepared natural polyphenolic bio-adhesives have excellent biocompatibility and degradability, which could be used for bio-adhesion *in vivo*.

3.5 Antioxidant and antibacterial ability of natural polyphenolic bio-adhesives

As natural polyphenolic bio-adhesives, which have excellent antioxidant properties, so the typical antioxidant tests (*i.e.*, 2,2-diphenyl-1-picrylhydrazyl (DPPH) and 2,2′-azinobis-(3-ethylbenzthiazoline-6-sulfonate) (ABTS) free radical testing) were carried out. As expected, the MTA natural bio-adhesives demonstrated an excellent free radical scavenging ability compared to MA due to unreacted hydroxyl groups contained in TA. For example, the scavenging rate of the MTA natural bio-adhesives in DPPH and ABTS free radical solutions after 30 min could reach ~90% and ~95%, respectively, (Fig. 6a and b). In addition, MA showed almost no obvious color change in the DPPH and ABTS solutions, and TA had an instantaneous color change, the MTA exhibited color changes over time, which further demonstrated that the MTA adhesives had excellent antioxidant properties (Fig. 6c and Fig. S10†).

Recently, phenolic networks were used for the treatment of bacterial infections and this has been widely reported.[26,52] For example, antimicrobial metal–phenolic network nanoparticles have been studied for use in wound healing, which identified that there were multiple antimicrobial modes of these polyphenolic NPs, including reactive oxygen species production, bacterial wall disruption, and quinoprotein formation.[53] So, the antibacterial properties of the MTA natural bio-adhesives were verified further. Firstly, the antibacterial activity of MA, TA, and MTA bio-adhesives was studied quantitatively using *S. aureus* and *E. coli* bacterial clearance. As shown in Fig. 6d and e, it was found that the survival rate of *E. coli* was 96.87%, 92.39%, 1.15%, and 3.29%, the survival rate of *S. aureus* was

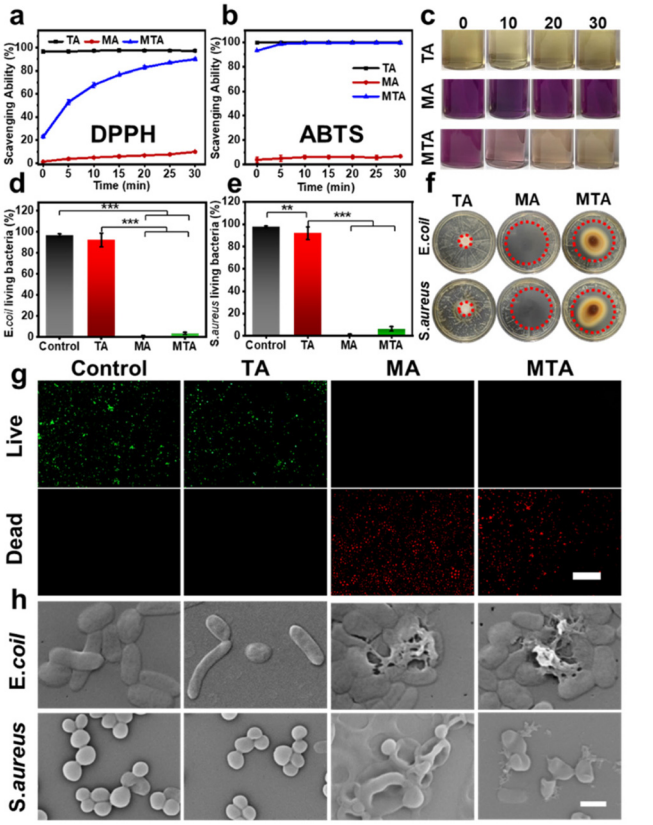

Fig. 6 Antioxidant and antibacterial abilities of natural polyphenolic bio-adhesives. (a) DPPH and (b) ABTS free radical scavenging abilities after different treatments. (c) Optical images of the color changes in DPPH free radical solution scavenged after different treatments. Antibacterial activity of different treatments against (d) *E. coli*, and (e) *S. aureus*. (f) The ZOI images of *E. coli* and *S. aureus* after different treatments. (g) Live/dead staining of S. *aureus* treated with different treatment groups (scale bar: 50 μm). (h) SEM images of *E. coli* and *S. aureus* after treatments with different groups (scale bar: 1 μm). (*$p < 0.05$, **$p < 0.01$, ***$p < 0.001$).

97.78%, 92.01%, 1.34%, and 6.23% after culturing with blank, TA, MA, and MTA natural bio-adhesives, respectively. In addition, the result of the ZOI experiment is shown in Fig. 6f, and both the MA and the MTA natural bioadhesives had obvious inhibition zones, which were consistent with the bacterial survival rates. Moreover, the live/dead bacteria staining tests showed that there were a lot of dead bacteria in the red staining in the MA and MTA natural bio-adhesives group, whereas the TA group and the control group had a lot of natural bacteria (Fig. 6g and Fig. S11†). In addition, it was observed by SEM, that the morphology of the bacteria was significantly changed after contact with each treatment group (Fig. 6h). The antibacterial activity of the MA and MTA natural bioadhesive would lead to bacterial aggregation and the destruction of the morphology. We believe that the mechanism of natural polyphenolic bio-adhesives mainly includes the bactericidal activity of natural extracts, as well as the multiple effects of the natural acid anhydride-polyphenol networks, including clearing the reactive oxygen species, inhibiting

protein formation, and destroying bacterial structures.[53,54] Above all, the MTA natural adhesives had excellent antioxidant and antibacterial properties, which could further enhance the healing of infected wound.

3.6 Natural polyphenolic bio-adhesives for bacterial infections wounds healing

To explore the antibacterial properties of MTA natural adhesives *in vivo*, the bio-evaluation in the rat bacterial infection wound healing model was performed. In brief, rat skin wounds with a length of 10 mm were prepared using a scalpel, and then bacteria (200 μL, 10^8 CFU mL^{-1}) was injected for 24 h. Next, the rats were randomly divided into four groups (surgical sutures, MTA adhesives, TA/MA powder, and control) and the appropriate treatments were applied to the wound, and the rats were fed normally, and the condition of the wounds was recorded at different times. As shown in Fig. 7a and b, it was found that the MTA-assisted groups exhibited faster healing and better wound healing of the infected mucosa when compared with other groups at different times. For example, the wound area of the untreated control, surgical sutures, TA/MA powder, and MTA adhesives reached 4.65 ± 0.39, 3.05 ± 0.61, 3.41 ± 1.05, 0.92 ± 0.18 mm^2 at day 8, respectively, which suggested that the MTA natural bioadhesives could perform better wound healing in bacterial and infectious environments (Fig. 7c). Noting that the number of bacteria obtained from wound culture treated with MTA bioadhesives and TA/MA powder gradually decreased after 2 days, which proved the long-lasting bacterial clearance ability in infected skin wound environments (Fig. 7d and Fig. S12†). In addition, the weight of the rats increased and the increased speed of healing with the MTA bioadhesives was faster than with the other groups, which further suggested that the MTA bioadhesives could showed better healing of infected wounds and a faster growth rate of the rats (Fig. 7e). Altogether, these results suggested that the MTA natural bioadhesives with natural extracts showed excellent bacterial infection wound healing ability.

Furthermore, various histopathological observations were conducted to evaluate the infected wound healing and the regenerative effects, including H&E staining, Masson's trichrome stain, platelet endothelial cell adhesion molecule-1 (CD31), tumor necrosis factor-alpha (TNF-α), IL-6, and Gram staining. As shown in Fig. 7f, the H&E staining revealed that the infected wound tissue treated with MTA bioadhesives exhibited higher levels of integrity and regularity when compared to the other test groups (Fig. S13a†). In addition, Masson's trichrome and CD-31 staining showed that the MTA bioadhesive treated group exhibited increased formation of collagen fibers and vessels in the wound healing area, which indicated that the MTA bioadhesives had a beneficial effect on infected wound healing (Fig. S13b†). Moreover, the inflammatory response TNF-α and IL-6 immunohistochemical staining showed that the positive expression of TNF-α and IL-6 in the wound treated with MTA bioadhesives was significantly reduced compared to the control group, which also indicated the good biocompatibility and lower inflammation of these natural polyphenolic bio-adhesives (Fig. 7g and Fig. S13c†). It was noted that the Gram staining showed that the MTA group showed lower bacterial expression, which further confirmed the excellent antibacterial performance of the MTA bioadhesives in infected wounds. Overall, these MTA bioadhesives could synergistically inhibit infected wound proliferation and inflammation, which could provide a new clinical strategy for the repair of other infected diseases.

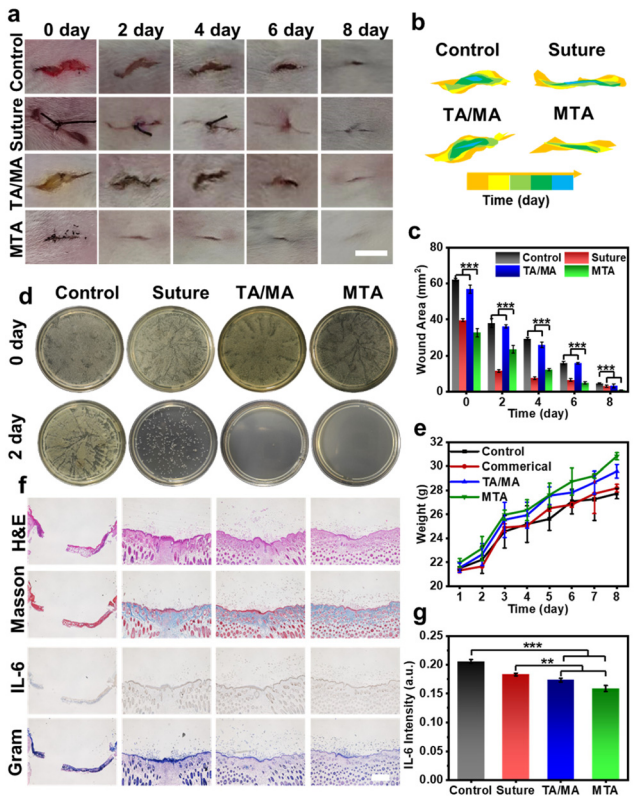

Fig. 7 Natural polyphenolic bio-adhesives for bacterial infected wound healing. (a) Representative photographs of wound areas at different times (scale bar: 10 mm). (b) Corresponding wound area simulated images of different groups. (c) Corresponding wound area statistics of different treatments. (d) Bacterial plate counting of different groups at different times. (e) Corresponding rat weight statistics of different treatments. (f) Representative histological H&E staining, Masson's trichrome, IL-6, and Gram staining after 8 days (scale bar: 50 μm). (g) Relative level of inflammatory responses of IL-6 staining after 8 days. (*p < 0.05, **p < 0.01, ***p < 0.001).

3.7 Natural polyphenolic bio-adhesives for hot burn infection wound healing

To further verify the multifunctionality of these MTA natural bioadhesives for infected wound healing, the bio-evaluation of a rat hot burn infection wound model was performed. In brief, the skin wound of rats was prepared with a hot metal stick, and ~100 μL of MTA bio-adhesive was dropped into the wound, and then pressed to produce adhesion. The control group did not have any treatment measures, and the commercial group applied the purchased commercial medicine dressing (Cofoe, G1308, China), then the rats were fed normally

and the wound area was photographed and recorded. As shown in Fig. 8a and b, it was also found that the MTA bioadhesive groups exhibited faster and better mucosal wound healing performances compared with the untreated control group, commercial medicine, and the TA/MA powder at different times. For example, the wound area of the untreated control group, commercial medicine, TA/MA powder, and MTA bioadhesives groups reached 26.17 ± 1.33, 11.85 ± 0.61, 5.24 ± 0.10, 1.45 ± 0.27 mm^2 at day 12, respectively, which suggested that the natural polyphenolic bio-adhesives could perform better wound healing in infected and bacterial environments (Fig. 8c). We also found that there were a lot of bacteria obtained from the wound culture, but they gradually decreased after treatment with the MTA bioadhesives and the TA/MA powder at different times, which proved the great bacterial clearance ability in the infected skin wound environment (Fig. 8d and Fig. S14†). In addition, the weight of the rats also increased and the increase speed of the MTA bioadhesives was faster than other groups, which further proved that the MTA bioadhesives could perform better infected wound healing, and showed a faster skin growth rate (Fig. 8e). Altogether, these results suggested that the MTA natural bioadhesives could perform excellent hot burn infection wound healing *via* a great adhesive and multifunctional performance.

Furthermore, various histopathological observations were also carried out to evaluate hot burn infection wound healing and regenerative effects. As shown in Fig. 8f and Fig. S15,† higher levels of integrity and regularity, more complete neoepidermis, and collagen fibers could be observed in the MTA natural adhesives compared to other groups at day 6 and day 12, which demonstrated that the MTA adhesive group could accelerate hot burn infected wound healing. From the TNF-α and IL-6 staining, it was found that a higher level of inflammation was detected in the wounds of control mice, but the infected wounds treated with MTA adhesives had a low level of inflammation (Fig. 8g and S16†). Next, Gram staining histological analysis was conducted to assess the bacterial status of the wounds after different treatments. It was found that the expression level in the MTA adhesives group was lower than that in the other groups, further confirming the excellent bacterial clearance ability of the MTA natural adhesives. Overall, we believe that these natural polyphenolic bio-adhesives could synergistically inhibit bacterial proliferation and inflammation, which could provide a new strategy for infected wound repair in clinical settings.

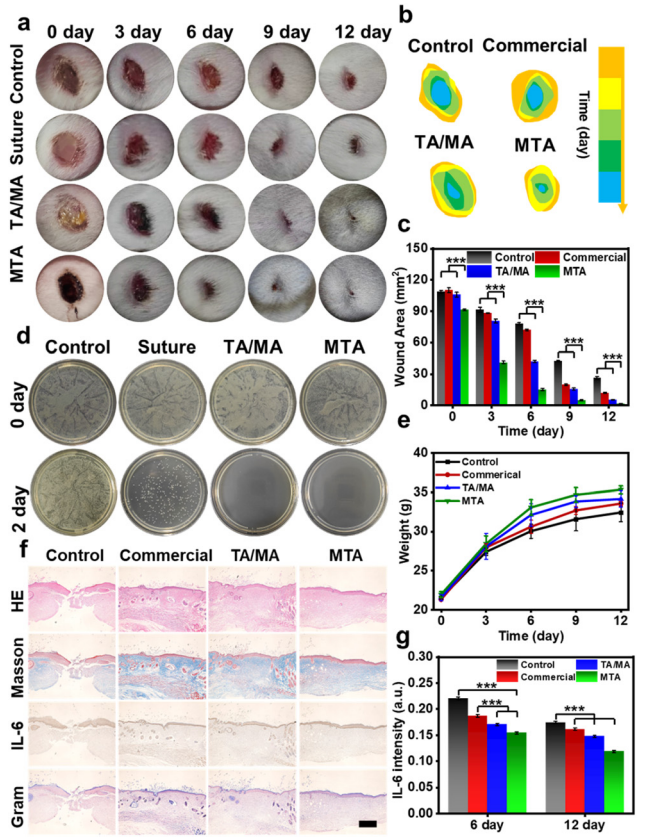

Fig. 8 Natural polyphenolic bio-adhesives for hot burn infected wound healing. (a) Representative photographs of hot burn infected wound area at different times (the diameter of the wound circle is 20 mm). (b) Corresponding hot burn infected wound area simulated images of different groups. (c) The corresponding hot burn infection wound area statistics of different treatments. (d) Bacterial plate counting of hot burn infected wound after different treatments. (e) Corresponding rat weight statistics after different treatments. (f) Representative histological images with H&E staining, Masson's trichrome, IL-6, and gram staining after 12 days (scale bar: 50 μm). (g) Relative level of inflammatory responses of IL-6 staining. (*p < 0.05, **p < 0.01, ***p < 0.001).

4. Conclusions

In summary, a series of natural polyphenolic bio-adhesives were prepared using the natural polyphenol and acid anhydride-crosslinking (PAC) reaction (acid anhydride ring opening and acylation reactions) between various natural polyphenols (extracts) and acid anhydrides. After heating, the natural polyphenolic adhesives could induce strong adhesion onto various substrates based on multi-interactions. Additionally, the as-prepared adhesives showed a rapid hemostatic performance, great biocompatibility, and appropriate biodegradability. In addition, the as-prepared natural bio-adhesives exhibited excellent antibacterial and anti-infective abilities, which could effectively promote bacterial infected wound healing and hot burn infected wound repair. We believe that this work could provide a new strategy for robust adhesion using naturally occurring molecules, and provide a method for the preparation of novel multifunctional wound dressings for infected wound healing.

Author contributions

The manuscript was written with contributions from all the authors. All the authors have given approval to the final version of the manuscript.

Conflicts of interest

The authors declare no conflict of interest.

Acknowledgements

This work was supported by supported by National Key R&D Program of China (No. 2022YFB3804400), the National Natural Science Foundation of China (No. 52173132), the Sichuan Science and Technology Program (No. 2023NSFSC1730), and the Fundamental Research Funds for Central Universities. All procedures using rats were approved by the Animal Care and Experiment Committee of West China Hospital of Stomatology affiliated with the School of Medicine, Sichuan University (WCHSIRB-D-2017-263).

References

1 Q. Pang, D. Lou, S. Li, G. Wang, B. Qiao, S. Dong, L. Ma, C. Gao and Z. Wu, *Adv. Sci.*, 2020, **7**, 1902673.
2 M. Mirhaj, S. Labbaf, M. Tavakoli and A. Seifalian, *Macromol. Biosci.*, 2022, **22**, 2200014.
3 P. P. Kalelkar, M. Riddick and A. J. García, *Nat. Rev. Mater.*, 2022, **7**, 39–54.
4 H. Ren, Z. Zhang, X. Cheng, Z. Zou, X. Chen and C. He, *Sci. Adv.*, 2023, **9**, eadh4327.
5 P. Du, Y. Shen, B. Zhang, S. Li, M. Gao, T. Wang, X. Ding, B. Yu, Z. G. Wang and F. J. Xu, *Adv. Sci.*, 2023, **10**, 2206851.
6 H. Hu and F.-J. Xu, *Biomater. Sci.*, 2020, **8**, 2084–2101.
7 L. Qiao, Y. Liang, J. Chen, Y. Huang, S. A. Alsareii, A. M. Alamri, F. A. Harraz and B. Guo, *Bioact. Mater.*, 2023, **30**, 129–141.
8 L. Yang, C. Wang, L. Li, F. Zhu, X. Ren, Q. Huang, Y. Cheng and Y. Li, *Adv. Funct. Mater.*, 2022, **32**, 2108749.
9 L. Miranda-Calderon, C. Yus, C. R. de Ganuza, M. Paesa, G. Landa, E. Tapia, E. Pérez, M. Perez, V. Sebastian and S. Irusta, *Chem. Eng. J.*, 2023, **476**, 146679.
10 H. Li, J. Zhang, L. Yang, H. Cao, Z. Yang, P. Yang, W. Zhang, Y. Li, X. Chen and Z. Gu, *Adv. Funct. Mater.*, 2023, **33**, 2212193.
11 H. Zhang, Q. Chen, J. Xie, Z. Cong, C. Cao, W. Zhang, D. Zhang, S. Chen, J. Gu and S. Deng, *Sci. Adv.*, 2023, **9**, eabn0771.
12 C. Chen, L. Chen, C. Mao, L. Jin, S. Wu, Y. Zheng, Z. Cui, Z. Li, Y. Zhang and S. Zhu, *Small*, 2023, 2306553.
13 L. Yang, L. Li, H. Li, T. Wang, X. Ren, Y. Cheng, Y. Li and Q. Huang, *Adv. Healthcare Mater.*, 2022, **11**, 2200112.
14 J. Yan, Y. Ji, M. Huang, T. Li, Y. Liu, S. Lu and M. Liu, *ACS Mater. Lett.*, 2020, **2**, 1375–1380.
15 G. Liu, Y. Zhou, Z. Xu, Z. Bao, L. Zheng and J. Wu, *Chin. Chem. Lett.*, 2023, **34**, 107705.
16 H. Zhang, J. Zhang, X. Peng, Z. Li, W. Bai, T. Wang, Z. Gu and Y. Li, *Adv. Sci.*, 2022, **9**, 2203587.
17 K. Lei, K. Wang, Y. Sun, Z. Zheng and X. Wang, *Adv. Funct. Mater.*, 2021, **31**, 2008010.
18 Z. Xu, G. Liu, L. Zheng and J. Wu, *Nano Res.*, 2023, **16**, 905–916.
19 M. Nakipoglu, A. Tezcaner, C. H. Contag, N. Annabi and N. Ashammakhi, *Adv. Mater.*, 2023, **35**, 2300840.
20 H. Zhang, Y. Xiao, P. Chen, H. Cao, W. Bai, Z. Yang, P. Yang, Y. Li and Z. Gu, *Biomacromolecules*, 2022, **23**, 3493–3504.
21 T. Wang, J. Zhao, Z. Yang, L. Xiong, L. Li, Z. Gu and Y. Li, *Green Chem.*, 2022, **24**, 3605–3622.
22 W. Zhao, X. Zhang, R. Zhang, K. Zhang, Y. Li and F.-J. Xu, *ACS Appl. Mater. Interfaces*, 2020, **12**, 56898–56907.
23 W. Tian, X. Wang, Y. Ye, W. Wu, Y. Wang, S. Jiang, J. Wang and X. Han, *Green Chem.*, 2023, **25**, 10304–10337.
24 Y. Xu, J. Hu, J. Hu, Y. Cheng, X. Chen, Z. Gu and Y. Li, *Prog. Polym. Sci.*, 2023, **146**, 101740.
25 Z. Li, Z. Chen, H. Chen, K. Chen, W. Tao, X.-K. Ouyang, L. Mei and X. Zeng, *Bioact. Mater.*, 2022, **17**, 49–70.
26 Y. Li, Y. Miao, L. Yang, Y. Zhao, K. Wu, Z. Lu, Z. Hu and J. Guo, *Adv. Sci.*, 2022, **9**, 2202684.
27 B. Hu, Y. Shen, J. Adamcik, P. Fischer, M. Schneider, M. J. Loessner and R. Mezzenga, *ACS Nano*, 2018, **12**, 3385–3396.
28 H. Geng, Z. Li, Z. Li, Y. Zhang, Z. Gao, L. Sun, X. Li, J. Cui, S. Ni and J. Hao, *Proc. Natl. Acad. Sci. U. S. A.*, 2023, **120**, e2220300120.
29 H. He, Q. Qin, F. Xu, Y. Chen, S. Rao, C. Wang, X. Jiang, X. Lu and C. Xie, *Sci. Adv.*, 2023, **9**, eadf3887.
30 Y. Liang, Z. Li, Y. Huang, R. Yu and B. Guo, *ACS Nano*, 2021, **15**, 7078–7093.
31 L. Yang, X. Zhang, J. Zhang, J. Hu, T. Zhang, Z. Gu and Y. Li, *Acta Polym. Sin.*, 2024, **55**, 192–201.
32 P. Yang, Q. Huang, J. Zhang, Y. Li, H. Gao and Z. Gu, *Adv. Mater.*, 2024, **36**, 2308393.
33 Y. Jiang, X. Zhang, W. Zhang, M. Wang, L. Yan, K. Wang, L. Han and X. Lu, *ACS Nano*, 2022, **16**, 8662–8676.
34 J. Sivasundarampillai, L. Youssef, T. Priemel, S. Mikulin, E. D. Eren, P. Zaslansky, F. Jehle and M. J. Harrington, *Science*, 2023, **382**, 829–834.
35 S.-H. Kim, K. Kim, B. S. Kim, Y.-H. An, U.-J. Lee, S.-H. Lee, S. L. Kim, B.-G. Kim and N. S. Hwang, *Biomaterials*, 2020, **242**, 119905.
36 C. Cui, C. Fan, Y. Wu, M. Xiao, T. Wu, D. Zhang, X. Chen, B. Liu, Z. Xu and B. Qu, *Adv. Mater.*, 2019, **31**, 1905761.
37 H. Cao, L. Yang, R. Tian, H. Wu, Z. Gu and Y. Li, *Chem. Soc. Rev.*, 2022, **51**, 4175–4198.
38 X. Shao, L. Su, J. Zhang, Z. Tian, N. Zhang, Y. Wang, H. Wang, X. Cui, X. Hou and T. Deng, *ACS Sustainable Chem. Eng.*, 2021, **9**, 14385–14394.
39 J. G. Hermens, A. Jensma and B. L. Feringa, *Angew. Chem., Int. Ed.*, 2022, **61**, e202112618.
40 T. Jin, H. Zeng, Y. Huang, L. Liu, D. Ji, H. Guo, S. Shi, G. Du and L. Zhang, *ACS Sustainable Chem. Eng.*, 2023, **11**, 11781–11789.

41 D. Zhang, K. Jin, K. H. Lim, S. Jie, W.-J. Wang and X. Yang, *Green Chem.*, 2023, **25**, 4696–4704.
42 C. Hu, X. Pang and X. Chen, *Macromolecules*, 2022, **55**, 1879–1893.
43 X. Xiao, M. Zhou, Z. Cong, L. Liu, J. Zou, Z. Ji, R. Cui, Y. Wu, H. Zhang and S. Chen, *CCS Chem.*, 2023, **5**, 994–1004.
44 H. Li, E. J. Cornel, Z. Fan and J. Du, *Chem. Sci.*, 2022, **13**, 14179–14190.
45 R. Zhou, Y. Wu, K. Chen, D. Zhang, Q. Chen, D. Zhang, Y. She, W. Zhang, L. Liu and Y. Zhu, *Adv. Mater.*, 2022, **34**, 2200464.
46 M. Huang, Y. Huang, H. Liu, Z. Tang, Y. Chen, Z. Huang, S. Xu, J. Du and B. Jia, *Biomater. Sci.*, 2022, **10**, 6413–6446.
47 H. Ye, Y. Xian, S. Li, C. Zhang and D. Wu, *Biomater. Sci.*, 2022, **10**, 4218–4227.
48 S. J. Wu and X. Zhao, *Chem. Rev.*, 2023, **123**, 14084–14118.
49 Y. F. Ma, J. X. Yao, Q. Liu, T. Han, J. P. Zhao, X. H. Ma, Y. M. Tong, G. R. Jin, K. Qu, B. Q. Li and F. Xu, *Adv. Funct. Mater.*, 2020, **30**, 2001820.
50 J. Park, E. Park, S. Q. Choi, J. Wu, J. Park, H. Lee, H. Kim, H. Lee and M. Seo, *JACS Au*, 2022, **2**, 1978–1988.
51 S. Guo, Y. Ren, R. Chang, Y. He, D. Zhang, F. Guan and M. Yao, *ACS Appl. Mater. Interfaces*, 2022, **14**, 34455–34469.
52 Y. J. Fu, Y. F. Shi, L. Y. Wang, Y. F. Zhao, R. K. Wang, K. Li, S. T. Zhang, X. J. Zha, W. Wang and X. Zhao, *Adv. Sci.*, 2023, **10**, 2206771.
53 R. Yu, H. Chen, J. He, Z. Zhang, J. Zhou, Q. Zheng, Z. Fu, C. Lu, Z. Lin and F. Caruso, *Adv. Mater.*, 2023, 2307680.
54 J. Bolaños-Cardet, D. Ruiz-Molina, V. J. Yuste and S. Suárez-García, *Chem. Eng. J.*, 2024, **481**, 148674.